



Influence of the Alkyl Chain Length on the Low Temperature Phase Transitions of Imidazolium Based Ionic Liquids

A. Cimini¹ · O. Palumbo¹ · F. Trequattrini^{1,2} · A. Paolone¹

Received: 30 January 2020 / Accepted: 21 March 2021 / Published online: 11 May 2021
© The Author(s), under exclusive licence to Springer Science+Business Media, LLC, part of Springer Nature 2021

Abstract

The effects induced by alkyl chain length on the thermal phase behavior for a series of imidazolium based ionic liquids (ILs) containing the anion bis(trifluoromethanesulfonyl)imide (TFSI) were investigated by infrared spectroscopy combined with density functional theory (DFT) calculations. In agreement with previous results on pyrrolidinium and ammonium based ionic liquids sharing the TFSI anion, our study shows that with increasing the length of the alkyl chain only the less stable *cis*-TFSI is retained in the solid state, while for shorter chain the *trans*-TFSI predominates in the crystalline phase. Also, we examined the remarkable effect on the packing efficiency due to the addition of 2-hydroxyethyl group on the imidazolium cation ring, reporting that the absence of crystallization is observed in correspondence with the presence of both the conformers of TFSI in the whole temperature range (150–325 K). Moreover, a detailed study of 1-ethyl-2,3-dimethylimidazolium-TFSI (EDMIM-TFSI) reveals the existence of cation rotational isomerism. In the liquid phase both *planar* (*P*) and *non-planar* (*Np*) conformers are present in the equilibrium, while a conformational change for the CNCC dihedral angle of the EDMIM cation leads to stabilize the formation of the more stable *non-planar* geometry in the crystalline phase.

Keywords Infrared spectroscopy · Ionic liquid · Rotational isomerism · Alkyl chain · Phase transitions

1 Introduction

Ionic liquids (ILs) are molten salts with melting temperature lower than 373 K and are typically composed of organic cations, such as pyrrolidinium, imidazolium, ammonium, or alkyl phosphonium, and organic/inorganic anions, like hexafluorophosphate (PF₆), tetrafluoroborate (BF₄), triflate (TfO), dicyanamide or tetracyanamethanide [1–4].

They are considered as promising safe electrolyte components for lithium batteries and, more broadly, for a wide variety of electrochemical devices; among various ILs the family of the pyrrolidinium cations and per(fluoroalkylsulfonyl)imide anions have received

✉ O. Palumbo
oriele.palumbo@roma1.infn.it

¹ CNR-ISC, U.O.S. La Sapienza, Piazzale A. Moro 5, 00185 Rome, Italy

² Dipartimento di Fisica, Sapienza Università di Roma, Piazzale A. Moro 5, 00185 Rome, Italy

special attention, due to the subambient melting temperature, high room temperature conductivity, and suitable electrochemical stability [5]. The physiochemical properties of the ionic liquids such as viscosity, electrical conductivity and glass transition temperature can be tuned by the selection of the suitable cation and anion. Understanding how combining ions can affect the specific anion–cation interaction is crucial to design new ionic liquids with desired properties. Modifications on the cation, including those with variation of the alkyl chain length or addition of the ether group to the N-alkyl chain, involve significant change in the macroscopic properties of the ILs.

Based on the analysis of diffusion NMR (Nuclear Magnetic Resonance) and SAXS (Small Angle X-ray Scattering) data, experimental evidence shows the effect of the cation alkyl chain size on the macroscopic transport properties for imidazolium-based ionic liquids [6]. Russina et al. [7] reported SWAXS (Small Angle and Wide Angle X-ray Scattering) measurements performed on 1-alkyl-3-methylimidazolium-TFSI ($C_n\text{mim-TFSI}$) with different alkyl chain length ($1 \leq n \leq 10$) providing evidence for the existence of nanoscale structural heterogeneities in the liquid phase whose size depends on the length of the alkyl chain and is related to chain segregation into nano-domains. X-Ray diffraction measurements as a function of temperature performed for 1-octyl-3-methylimidazolium tetrafluoroborate ($C_8\text{mim-BF}_4$) showed the presence both in the liquid and in the supercooled state of nanostructural organization as a consequence of the strong and isotropic Coulombic interaction between the anion and the charged imidazolium ring [8]. Previous work [9] reports that the presence of an ether oxygen in the alkyl side chain contributes to suppress the crystallization of ILs. Indeed, for various ether-functionalized ILs the values of the melting temperature, T_m , can be reduced compared to those observed for ionic liquids, which do not present any ether group [10]. Conversely, the presence of the ether oxygen increases the polarity, which improves the interionic interactions in the packing state, thus increasing the T_m of ILs [11]. These indications suggest that a compromise of these effects, namely the increase in polarity and flexibility, plays a key role to understand the microscopic change occurring across the melting. Moreover, different conformation features and alteration of the intermolecular interaction can affect the physical and chemical properties of the ILs. Investigations [12] at different compression rate on 1-ethyl-3-methylimidazolium trifluoromethanesulfonate (EMIM- CF_3SO_3) report that weak interaction may lead to different crystalline polymorphs in relationship with conformation isomerism of the EMIM cation. Previous investigations on pressure induced phase transitions in relation to cation conformational isomerism were performed on several 1-ethyl-3-methylimidazolium based ionic liquids. It was noted that *planar* and *non-planar* configurations coexist in the liquid state under ambient pressure and temperature, although an increase in pressure appears to induce rotational isomerism of the ethyl group by promoting the *planar* geometry in the crystalline state [13–15].

In this framework, the knowledge of the different conformers distribution and their evolution in the different physical states provides useful information. The infrared spectroscopy is a powerful tool to probe the different microscopic configurations of the ions and the evolution of their concentration as a function of temperature or pressure. We investigated [16–24] by means of this technique several ILs sharing a common TFSI anion observing that significant change in the molecular geometry occurs at the phase transitions. This flexible ion shows two energetically inequivalent conformations, the *cisoid* (*cis*) and *transoid* (*trans*) forms, whose concentration affects the ILs physical and chemical properties both in the solid and liquid phases. The *transoid* conformer with the C_2 symmetry results to be more stable than the *cisoid* one, which has a C_1 symmetry; however due to a low energy separation ($\sim 2.2 \text{ kJ}\cdot\text{mol}^{-1}$) both conformers are present in the liquid phase [25, 26]. In

recent studies we showed from an analysis of the infrared absorption spectra performed on trimethyl-*N*-hexylammonium-TFSI (TMHA-TFSI) and *N*-trimethyl-*N*-propylammonium-TFSI (TMPA-TFSI) that different lengths of the cation alkyl chain in these ammonium based-ILs induce different relative concentration of the anion conformers in the solid phase [17]. Indeed, in solid TMPA-TFSI the relative concentration of the TFSI is shifted toward the predominance of the *transoid* conformer, in accordance to that observed for other ILs containing the TFSI anion, where only this lowest energy rotamer survives in the crystalline state [16–21]. Conversely, the solid TMHA-TFSI, with a longer chain, promotes the formation of the less thermodynamically stable *cis* geometry. We found a similar behavior analyzing the infrared spectrum and its temperature dependence for a series of pyrrolidinium PYR_{1A} based ionic liquids sharing the TFSI anion (with A ranging between 3 and 8) displaying that longer alkyl chain, starting from a threshold value of $A \sim 6$, induces the system to stabilize the *cis* geometry in the solid phase [22]. This implication could be correlated to the capacity of the ILs to assume tail-segregated conformations in nanodomains [7, 8, 27, 28], resulting in different structural ordering for the anion molecules in the solid state. However, the cations taken into consideration such as ammonium and pyrrolidinium include a considerably number of bonds around which different rotation can provide geometric isomers, so that they could alter the interionic interaction in the system; the obtained results suggest that the conformational change occurring to the TFSI anion in the different phases can be mainly attributed to the alkyl chain length effect. These experimental observations require further investigation to get insight into the role of the cation alkyl chain on the intramolecular rearrangements of the anion conformers.

In this work, we extend our study on imidazolium-based ionic liquids sharing the same TFSI anion but differing in aliphatic side chain length: 1-ethyl-2,3-dimethylimidazolium-TFSI (EDMIM-TFSI), 1-hexyl-3-methylimidazolium-TFSI (HMIM-TFSI) and 1-ethanol-3-methylimidazolium-TFSI (HOEMIM-TFSI). By combining infrared spectroscopy technique and DFT calculations of the vibration frequencies of the single ions composing the ILs, we are able to detect the different conformers and to ascertain the evolution of their relative concentration with the temperature. The measured spectra for these ILs confirm the important role of the alkyl side chain on the stabilization of the TFSI anion in either the *trans* or the *cis* configuration upon the occurrence of phase transitions. Accordingly, the HMIM-TFSI retains the less thermodynamically stable *cis* conformer in the solid phase, whereas EDMIM-TFSI adopts the *trans* configuration. Concerning the HOEMIM-TFSI, which contains an alcohol $(\text{CH}_2)_2\text{OH}$ as a functional group in the imidazolium ring, our study provides new information about thermodynamic behavior changes of imidazolium salts associated with the functionalized chain. In addition, by the present measurements performed on EDMIM-TFSI and compared with DFT calculation, we observe that alkyl chain rotation on the imidazolium ring lead to stabilize the *non-planar* configuration at the equilibrium in the crystalline phase, proving the existence of rotational isomerisms for EDMIM cation.

2 Experimental

Three ionic liquids were investigated in the present work. The EDMIM-TFSI and HMIM-TFSI were purchased from Iolitec Inc. The purity of these samples was 99% and no further purification was used before measurements. HOEMIM-TFSI (99.5%) was purchased from Solvionic and used as received. All samples were heated at around 80 °C overnight in

vacuum to remove undesired water. Infrared spectroscopy measurements were performed by means of a Bruker IFS125 HR spectrometer at the AILES beamline of the SOLEIL Synchrotron [29, 30]. The spectra were recorded in the mid-infrared at a resolution of 0.5 cm^{-1} , by combining a KBr beamsplitter and an MCT detector. Thin layers of ILs were dropped between two diamond windows and then placed in a heatable optical cell closed by means of viton O-rings to avoid contamination from air. The transmission measurements were calculated using the spectrum of the bare optical windows as reference and they were subsequently converted to absorbance data. The samples were cooled down to 140 K by means a Cryomec cryopump with a temperature rate of $\sim 5\text{ K}\cdot\text{min}^{-1}$, and data were collected on heating at the same rate between this minimum temperature and 325 K.

3 Computational

Calculations were performed using the Spartan software to find preliminary geometries of EDMIM, HMIM, HOEMIM and TFSI ions at the force field level (MMFF) [31, 32]. A systematic search of conformers was performed at this level, rotating the flexible CC bonds by 120° . For TFSI, HOEMIM and HMIM we obtained 2, 2 and 69 possible structures. Afterwards, the geometry of the obtained conformers was optimized using DFT calculations with the 6-31G** basis set and the B3LYP functional. Finally the vibrational frequencies and the IR intensities were calculated at the same level of DFT theory and basis set. Only the structures with all positive frequencies were considered in the following. The combination of the 6-31G** basis set and the B3LYP theory has been frequently used in the literature to investigate the vibrational properties of the ILs [25, 32–34]. The IR spectrum of each conformer was simulated by summing Gaussian curves centered at each calculated IR vibration frequencies with a fixed 10 cm^{-1} peak width [16].

For comparison purposes, the geometry of relevant conformers was optimized also at the MP2 level of theory, using the aug-cc-pVDZ basis set. However, as the computed vibration frequencies have a poorer agreement with the experiments than the B3LYP/6-31G** results, they are reported in the Supplementing Information file and in the following the calculations based on B3LYP DFT will be used for the attribution of the experimental absorption bands.

3.1 Computational Results

The conformational analysis performed by means of the Spartan software on the three samples investigated shows that HMIM ion possesses six possible stable conformers, labelled as $C_i = 1, 2, 3, 4, 5$, while the HOEMIM ion provides only two stable configurations labeled as $C_i = 1, 2$ shown in Fig. 1.

All other conformers that were found to have energy difference higher than $5\text{ kJ}\cdot\text{mol}^{-1}$ from the conformer of lower energy (C_1) were not considered in the following since at ambient temperature the population for these states occurs in negligible quantities. Non stable configurations were of course not considered. While for HMIM and HEOMIM the calculations performed by Spartan can successfully identify possible conformers, in the case of EDMIM a more complex procedure should be adopted, as already performed in the literature in the case of the EMIM cation [35]. Indeed, for the case of EDMIM an investigation of the energy as a function of the torsion angle between the imidazolium plane and the ethyl group were performed. A previous work [35], reports a similar calculation,

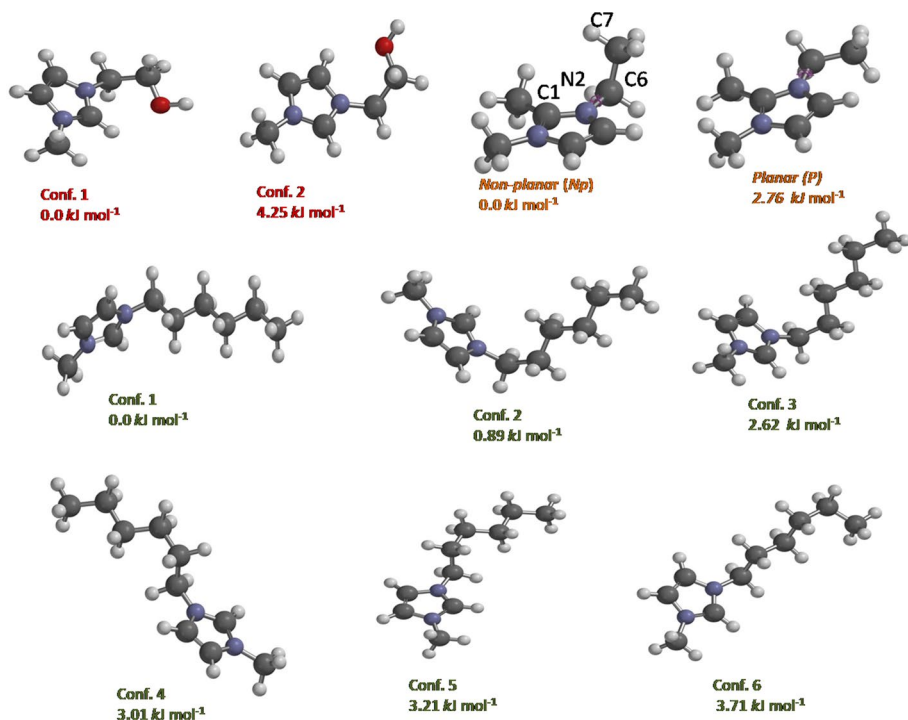


Fig. 1 Schematic of the optimized structures: 1-ethanol-3-methylimidazolium (HOEMIM) (red), 1-ethyl-2,3-dimethylimidazolium (EDMIM) (orange) and 1-hexyl-3-methylimidazolium (HMIM) (green). The nitrogen atom is drawn in purple while the carbon, hydrogen and oxygen atoms are colored in gray, white and red respectively. The number indicates the energy difference respect to the lowest energy conformer

where the energy profile calculated as a function of the dihedral angle that the EMIM cation formed between the imidazolium plane and the CH_3 group of the alkyl chain, by using different basis sets at the B3LYP, MP2 and HF level theory and displays that the ethyl group rotation along the C–N bond determines two local minima situated at angles of 110° and 0° , which correspond to *non-planar* and *planar* conformers respectively. Furthermore, the comparison between vibrations calculated for both optimized geometries and the experimental spectroscopic measurements performed on several ionic liquids containing 1-ethyl-methyl-imidazolium ion confirmed the existence of these conformers in the liquid phase thus providing a validation of the computational approach [13, 15, 35]. The energy profile as a function of the CNCC dihedral angle of the EDMIM cation obtained from the DFT calculations by the B3LYP functional with the 6-31G** basis set for rotations of 10° is reported in Fig. 2.

The relative energy, ΔE , is calculated from the most stable conformer, which is found at $\sim 90^\circ$ and corresponds to the *non-planar* (*Np*) geometry. It is noted that the same configuration with regard both to energy and spatial arrangements occurs also at -90° as a result of the rotational symmetry above the imidazolium plane. A local minima, with an energy higher by $\Delta E \sim 2.76 \text{ kJ}\cdot\text{mol}^{-1}$ with respect to the *non-planar* one was found at a dihedral angle of $\approx 180^\circ$ and represents the *planar* (*P*) configuration (see Fig. 1), where the ethyl chain is on the plane of the cation ring, on the opposite side of the methyl group on the

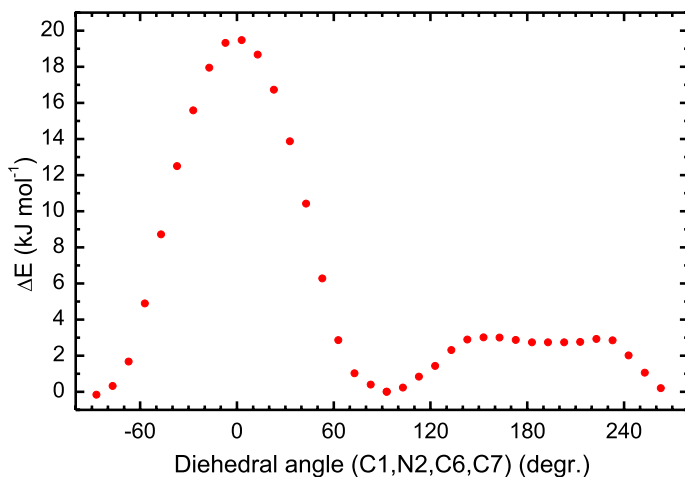


Fig. 2 Calculated torsion energy profile for the C1-N2-C6-C7 (see Fig. 2) dihedral angle of EDMIM ion using the DFT calculation at B3LYP level of theory with 6-31G** basis set

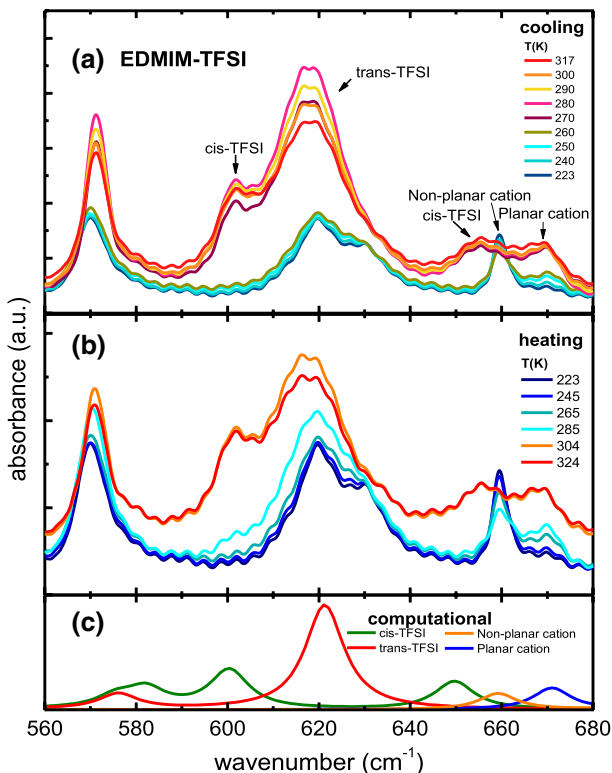
carbon atom. Instead, as it can be seen in Fig. 2, the proximity between the alkyl chain and the methyl group leads to increase the relative energy, probably due to the electrostatic repulsion effect, thus providing a maximum situated at 0° , for which an unstable structure occurs, as witnessed by an imaginary frequency in the vibrational spectrum. As the torsion energy profile indicates, the dihedral angles for which the alkyl side chain results perpendicular to the imidazolium ring provides conformers with lower energy than those presenting a planar geometry. The computational analysis carried out on EDMIM ion shows that ethyl group rotation can involve the formation of the *planar* stable conformer for dihedral angle equal to 180° as well as the *non-planar* one, which occurs for dihedral angle equal to 90° and is favored in energy (see Fig. 1). The vibrational frequencies and the infrared intensity of all conformers considered for the three cations are reported in the Supplementing Information.

4 Results and Discussion

The temperature dependence of the infrared spectrum ($560\text{--}680\text{ cm}^{-1}$) of EDMIM-TFSI in the range between 324 and 223 K is reported in Fig. 3a on cooling and Fig. 3b during the subsequent heating.

This frequency range contains the markers of both the anion and cation conformers. Indeed, the lines observed at ~ 602 and $\sim 655\text{ cm}^{-1}$ are ascribed to *cis*-TFSI while that at $\sim 618\text{ cm}^{-1}$ is due to *trans*-TFSI [16, 25, 26]. At room temperature, in the liquid state both the anion conformers are present. On cooling, the intensity of the lines observed at 602 and 655 cm^{-1} of the *cis* isomer drastically decreases and they disappear completely for temperature values close to $\sim 260\text{ K}$, indicating the occurrence of a phase transition towards a solid state, with a strong predominance of the *trans* rotamer. This behavior is consistent with the occurrence of only the *trans* conformer of TFSI in most solids containing this anion [16–21]. Furthermore, the disappearance of the line centered at 655 cm^{-1} below the crystallization temperature makes it possible to observe two bands centered at ~ 660 and

Fig. 3 Temperature dependence of the absorbance of sample EDMIM-TFSI measured on cooling (a) and subsequently on heating (b). All the measured spectra were compared with calculated infrared spectra (c) of the isolated anion and cation conformers. A frequency scaling factor lower than one (0.981) was adopted for the cation conformers in the frequency region concerned

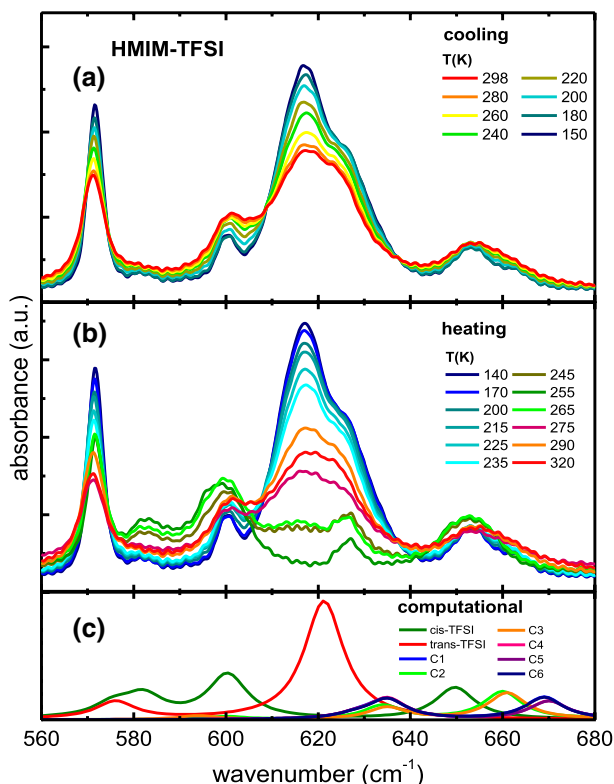


$\sim 669 \text{ cm}^{-1}$, that can be attributed to the *non-planar* (*Np*) and *planar* (*P*) cation conformers, respectively, as suggested by the comparison with the DFT simulation (Fig. 3c). Indeed, in the liquid state the line at 655 cm^{-1} due to the *cis*-TFSI ion is superimposed on the absorptions due to the cation conformers and this superposition makes it difficult to identify the peak at 660 cm^{-1} . In the solid phase, the intensity of the absorbance peak at 660 cm^{-1} due to the *Np* isomer of the cation tends to increase at lower temperature while the intensity of the line centered at 669 cm^{-1} attributed to the *P* conformer decreases, indicating a drastic cation configuration change. Moreover, on heating (Fig. 3b) around $\sim 290 \text{ K}$, the narrow peak at 660 cm^{-1} disappears, the small band centered at 669 cm^{-1} due to the *P*-cation becomes more intense and the large band at $\approx 650 \text{ cm}^{-1}$ due to the *cis* conformer of the anion reappears: this behavior can be ascribed to the occurrence of the melting process.

The temperature dependence of the infrared absorption spectrum of sample HMIM-TFSI is reported in Fig. 4.

On cooling down to 150 K the well-known bands centered at ~ 600 , 653 and 616 cm^{-1} due to the presence of both *cis* and *trans*-TFSI respectively become narrower and the central peak increases in intensity, indicating the lack of crystallization at low temperatures. More precisely, the absence of abrupt changes in the absorbance, which displays only a monotonous and continuous behavior with the temperature, rather suggests that the liquid undergoes a glass transition. This conclusion is also in agreement with previous experimental heat capacities measurements performed on HMIM-TFSI in the range $5\text{--}310 \text{ K}$, where a glass transition was found around 180 K for this liquid [36, 37].

Fig. 4 Temperature dependence of the absorbance of sample HMIM-TFSI measured on cooling (a) and subsequently on heating (b). All the measured spectra were compared with calculated infrared spectra (c) of the isolated anion (*cis* and *trans* conformers) and cation (C1, C2, C3, C4, C5 and C6 conformers)



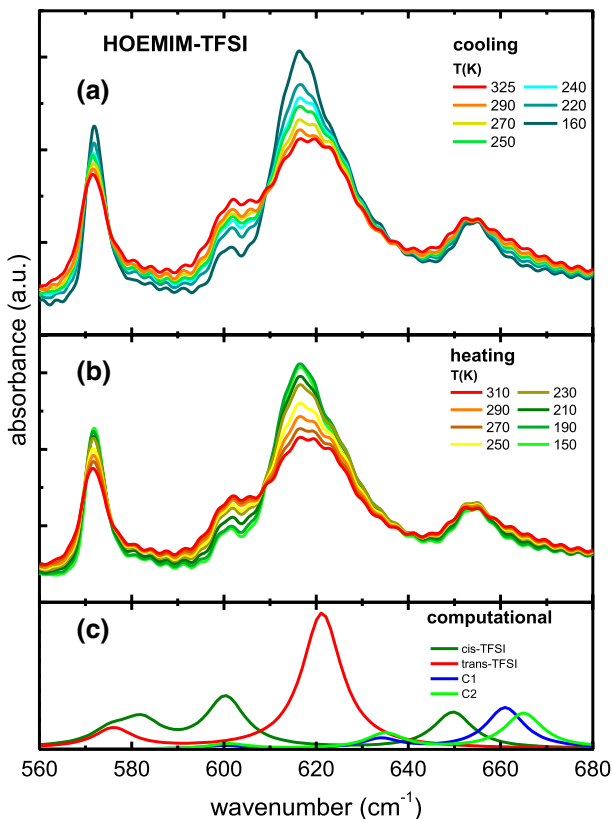
On heating, the intensity of the line at about 616 cm^{-1} monotonously decreases and suddenly disappears when the system possibly enters into a cold crystallized phase ($\sim 245 \text{ K}$). Instead, around this temperature the lines at 600 and 653 cm^{-1} are both well detectable indicating that the HMIM-TFSI retains only the less-stable *cis*-TFSI conformer in the solid phase. Moreover, the disappearing of the line at 616 cm^{-1} attributed to the *trans* conformer allows the clearly detection of a line at 626 cm^{-1} , which in the liquid phase (and likely also in the glass phase) appears as a shoulder of such line.

The comparison with the simulations reported in Fig. 4c suggests that this line at 626 cm^{-1} is related to some vibrational modes of the cation. Heating up HMIM-TFSI ($\sim 270 \text{ K}$), the intensity of the lines centered at 600 and 653 cm^{-1} of the *cis* isomer begins to decrease, while the absorption at 616 cm^{-1} , attributed to *trans*-TFSI, reappears increasing its intensity considerably. These facts suggest the occurrence of melting around 270 K .

The evolution of the infrared spectrum ($650\text{--}680 \text{ cm}^{-1}$) of sample HOEMIM-TFSI as a function of temperature is reported in Fig. 5.

The three lines at 600 , 616 and 654 cm^{-1} are present in the whole temperature range, both on cooling and heating (Fig. 5a and b), indicating the simultaneous presence of both TFSI conformers at all temperatures. As observed before for HMIM-TFSI sample, no signature of the occurrence of crystalline phase transition is observed in the spectra measured on cooling HOEMIM-TFSI sample. Indeed, on cooling, the intensity of the central band around 616 cm^{-1} , attributed to the *trans* anion conformer, keeps growing down to lower temperatures ($\sim 160 \text{ K}$) while the intensities of the side bands at 600 and 654 cm^{-1}

Fig. 5 Temperature dependence of the absorbance of sample HOEMIM-TFSI measured on cooling (a) and subsequently on heating (b). All the measured spectra were compared with calculated infrared spectra (c) of the isolated anion (*cis* and *trans* conformers) and cation (C1 and C2 conformers)



of the *cis* isomer decrease. Conversely, on heating back, the *trans* peak at about 616 cm^{-1} monotonously decreases, whereas the *cis* peaks around 600 and 654 cm^{-1} become wider and increase in intensity up to 310 K, suggesting that both the *transoid* and *cisoid* configurations of TFSI anion are populated in the liquid phase. This fact linked to the intensity of the bands indicates that this sample does not crystallize, neither on cooling nor on the subsequent heating and therefore it most likely transforms into a glass at low temperature. These observations will be further corroborated in the following by a quantitative analysis of the relative concentration of the TFSI conformers as a function of temperature.

These results clearly show that the configurations assumed by the TFSI anion in the different states are strictly influenced by the length of the cation alkyl chain. We observed for all the three samples that in the liquid phase, both the *cis*- and *trans*-TFSI conformers are present. Nevertheless, at low temperatures the samples undergo different phase transitions: EDMIM-TFSI, with shorter alkyl side chain, crystallizes on cooling and in the solid phase it retains only the *trans* anion conformer; HMIM-TFSI, with longer alkyl chain, undergoes a glass transition upon cooling and it cold crystallizes in the subsequent heating, retaining in the solid phase only the less thermodynamically stable *cis* anion rotamer; finally, HOEMIM-TFSI exhibits the presence of both TFSI conformers at all temperatures, suggesting that it never crystallizes but, more likely, it transforms into a glass at low temperatures.

More indications about the occurrence of a liquid, glassy or crystalline phase can be obtained by a quantitative analysis of the IR spectrum, which provides a detailed picture of

the temperature evolution of the conformers in the samples [16–21, 24]. Indeed, the ratio of the intensities, r , of peaks attributable to the different rotamers is proportional to the relative concentration:

$$r = \frac{I_{\text{cis}}}{I_{\text{trans}}} = \frac{[C_{\text{cis}}]}{[C_{\text{trans}}]}, \quad (1)$$

where I_x indicated the integrated IR intensities of the band centered at wavenumber x [17, 18, 20, 24] after subtraction of a background. In the previous formula any difference in the molar absorptivities of the two conformers is not considered and the absorptivity of each of them is considered temperature-independent. In the present case, it was calculated as:

$$r = \frac{I_{\text{cis}}}{I_{\text{trans}}} = \frac{I_{602}}{I_{618}}. \quad (2)$$

It can be observed that in the liquid state the relative concentration of the two conformers of TFSI follows the Boltzmann law, which lead to the following Van't Hoff equation:

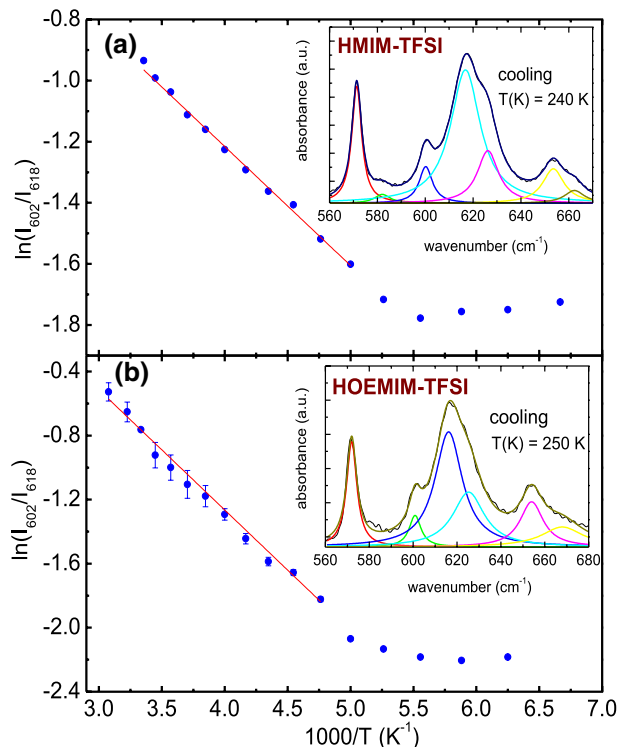
$$\ln(r) = -\frac{1}{T} \frac{\Delta H}{R} + \frac{\Delta S}{R} + c, \quad (3)$$

where ΔH and ΔS are the enthalpy and entropy difference between the two TFSI conformers. On entering the glass state, the distribution of the conformers population is completely frozen and the quantity $\ln(r)$ does not depend on the temperature [17, 18, 24]. The ratio of the relative conformer concentration, r , was determined by using the intensities of the bands at 602 and 618 cm^{-1} of the *cis* and *trans* conformer respectively, whereas the *cis* peak at $\sim 655 \text{ cm}^{-1}$ was not considered because it overlaps with the absorptions due to the cation conformers, which were observed in the experimental spectra ranging between 640 and 680 cm^{-1} for all samples. In order to obtain the intensities of these bands, the spectra measured on cooling for each of the three samples were deconvoluted into several peaks taking into account the contributions coming from the shared TFSI anion, three centered at 602, 618 and 655 cm^{-1} and the one at 570 cm^{-1} as well as to the contributions due to the different imidazolium cations.

In particular, the experimental spectra of HMIM-TFSI were deconvoluted in the frequency range between (560–680 cm^{-1}) using seven Lorentzian peaks, four of which are attributed to the vibrational modes of TFSI at 600, 616, 653 and 570 cm^{-1} and three were used to account for the cation conformers.

Concerning the HOEMIM-TFSI, the intensities of the bands were obtained by fitting the absorbance spectra in the same frequency range (560–680 cm^{-1}) with six Lorentzian peaks, one for each of the four bands corresponding the TFSI conformers absorptions and two centered at 624 and 668 cm^{-1} corresponding to vibrational modes, which can be due either to C1 or C2 cation conformations, as can be seen from the computational results (Fig. 5c). With regard to EDMIM-TFSI sample, the intense absorption peaks observed at 570, 602 and 618 cm^{-1} due to the anion were fitted with three different Lorentzian peaks, whereas three more peaks were used to reproduce the bands centered at 660 and 669 cm^{-1} , attributed to different vibrational modes of *non-planar* and *planar* cation conformers respectively, and the one at 655 cm^{-1} due to the vibration band of *cis* rotamer. Plots of the $\ln(r)$ vs. $1/T$ for HMIM-TFSI and HOEMIM-TFSI are reported in (a) and (b) in Fig. 6 respectively, with an example of the fit of the absorbance spectrum. The linear behavior of the $\ln(r)$ at higher temperatures reflects, in the liquid phase, the temperature dependence of the concentrations for the two distinct conformers

Fig. 6 Temperature dependence (on cooling) of the logarithm of the ratio of the intensities of the bands due to the *transoid* and *cisoid* TFSI conformers for **a** HMIM-TFSI and **b** HOEMIM-TFSI. The insets report two examples of the deconvolution of the spectra



of the TFSI whereas the flat slope, which is observed down to low temperatures, provides a clearly indication of the glass transition temperature, that occurs at around 198 and 186 K for the HOEMIM-TFSI and HMIM-TFSI respectively. This latter value is comparable with the glass transition temperature ($T=183$ K) detected in other works [36, 37]. Indeed, the evident change in slope of $\ln(r)$ corresponds to an almost constant concentration of the two conformers of TFSI below the glass transition temperature. This suggests a freezing of the distribution of the conformer populations entering in the glass state indicating that the relative concentrations of the *cis* and *trans* TFSI does not change any longer for temperatures below the glass transition. This result is in agreement with the expected lack of dynamics on short time scales in the glass phase. The enthalpy difference values, derived from the linear regression of $\ln(r)$ vs. $1/T$ in Fig. 6, are equal to $\Delta H = 3.24 \pm 0.06$ $\text{kJ}\cdot\text{mol}^{-1}$ and $\Delta H = 6.26 \pm 0.08$ $\text{kJ}\cdot\text{mol}^{-1}$ for the HMIM-TFSI and HOEMIM-TFSI respectively and are compatible with the ones reported for other ILs containing the TFSI anion, which range between 3 and 7.3 $\text{kJ}\cdot\text{mol}^{-1}$ [18, 22–24, 26, 38]. In particular, the ΔH value here obtained for the HMIM-TFSI is consistent with the enthalpy difference estimated from the analysis of the temperature dependence $I_{\text{cis}}/I_{\text{trans}}$ intensity ratios derived from the reduced isotropic spectra values for the same sample (3.86 ± 0.66 $\text{kJ}\cdot\text{mol}^{-1}$) [39].

In Fig. 7a the plot of $\ln(r)$ vs. $1/T$ for the conformers of the anion for EDMIM-TFSI is reported in the temperature range between 320 and 270 K, corresponding to the liquid phase. The quantity $\ln(r)$ cannot be calculated upon the occurrence of the phase transition from liquid to solid due to the disappearance of the *cis* band at 602 cm^{-1} . The

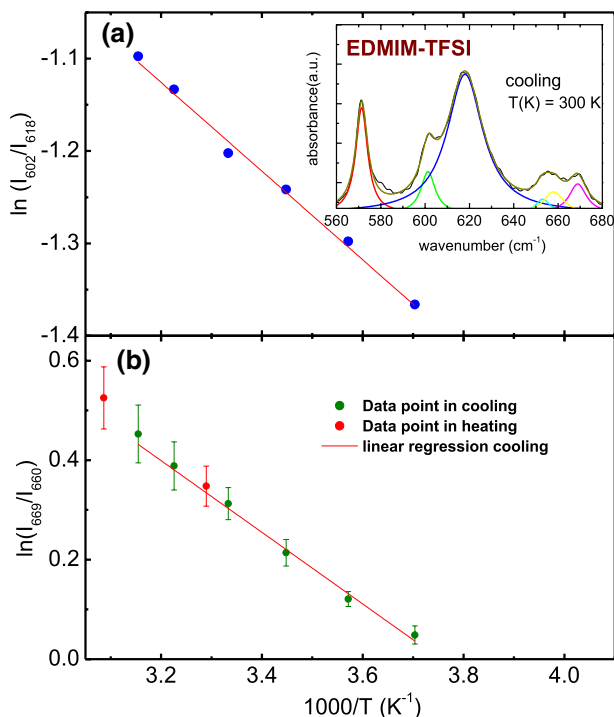


Fig. 7 Temperature dependence of the logarithm of the ratio of the intensities of the bands due to the *trans*- and *cisoid* TFSI conformers in **a** on cooling EDMIM-TFSI. Van't Hoff plot (**b**) of the calculated $\ln(r)$ value for the conformers of the EDMIM cation

slope of the plot provides the ΔH between the two TFSI conformers, which is equal to 3.99 ± 0.37 kJ·mol⁻¹ and is compatible with the previous estimated values of the other samples. The positive value of the enthalpy difference, ΔH , indicates that the concentration of the conformers tends to favor the thermodynamically stable rotamer, the *trans* on cooling, whereas in the liquid phase both configurations of the TFSI are found in a dynamic equilibrium.

Summarizing the results reported so far, we can conclude that at the used temperature rate both HMIM-TFSI and EDMIM-TFSI display a crystalline phase at low temperatures, however different spatial arrangements of the TFSI anion were observed for these two compounds. The presence of the unstable *cis* rotamer in the solid HMIM-TFSI is quite unusual and has been observed only for a few other ionic liquids having different cations involving long enough alkyl chain: Vitucci et al. [17] suggested that the presence of *cis* rotamer in the solid phase of TMHA-TFSI could be explained by a stronger cation–anion interaction compared to that experienced between the TFSI and the shorter chain TMPA cation; in a recent study we reported the infrared spectra measured for a series of pyrrolidinium PYR_{1A} based ionic liquids sharing the TFSI anion showing that an increase of the length on the cation alkyl chain ($6 \leq A \leq 8$) favored the less-stable *cis*-conformer in the solid phase, by means of a different balance of forces between the two oppositely charged ions. In previous studies, the occurrence of *cis*-TFSI in the crystalline phase was reported in two imidazolium based ionic liquids: 1,3-dimethylimidazolium [40] and 1-ethyl-3-methylimidazolium

[41]. Raman spectroscopy investigation showed that the crystalline 1-ethyl-3-methylimidazolium TFSI retains the *cis* isomer after fast cooling ($\sim 20 \text{ K}\cdot\text{min}^{-1}$) relative to the thermodynamically stable *trans* rotamer, which on the other hand is the only one that prevails after a slow cooling rate of $\sim 1 \text{ K}\cdot\text{min}^{-1}$ [42].

Based on the experimental evidence from infrared spectroscopy, reported in this work and observations made above about previous investigation performed on imidazolium, ammonium and pyrrolidinium based ionic liquids sharing the TFSI anion, we suggest that the different alkyl side chain length affects the interactions in these structured liquids inducing different behavior in the solid state. In particular, for these ionic liquids an increase of the alkyl chain length slows down the crystallization kinetics and tends to stabilize the *cis* conformer of highest energy in the solid phase.

Additional considerations can be herein introduced, considering the effect of the alcohol group on the physicochemical properties of imidazolium based ILs. It was observed [43, 44] that high polarity behavior shown from hydroxyl ILs is correlated to an increase of intermolecular interactions, even suggesting that the well-known hydrogen bonding occurring between anion and $\text{C}_2\text{-H}$ site on the imidazolium ring is replaced by a stronger one involving the hydroxyl group $-\text{OH}$ on the side chain. This is supported also by the optimized structures calculated [45] for isolated and dimer ion pairs of C_2OHmim cation and different anions, including BF_4^- , PF_6^- , CF_3SO_3^- , TFSI^- , where it is noted that the hydroxyl group provides a strong site to interact by means of hydrogen bonds with the anion, thus affecting the ion packing efficiency in all selected ILs. The glassy state observed on cooling and subsequently heating the HOEMIM-TFSI may be caused by the flexibility of the ethanol side chain that strongly affects the distribution of the anion conformers, not allowing the system to crystallize, thus extending the temperature range of the liquid state. Such a behavior, that is the lack of a liquid–solid transition, was observed also investigating symmetric and asymmetric non-hydroxyl ionic liquids like 1,3-dialkylimidazolium ($(\text{C}_{\text{N}/2})_2\text{im-TFSI}$) and 1-alkyl-3-methylimidazolium ($\text{C}_{\text{N}-1}\text{C}_1\text{im-TFSI}$), respectively, by showing that longer alkyl chains and asymmetry ($\text{N}=8$ and 10) hinder the crystallization, therefore only a glass transition was observed [28]. As seen above, by comparing the temperature dependence of the infrared spectra of EDMIM-TFSI ($560\text{--}680 \text{ cm}^{-1}$) with the DFT calculation it was possible to attribute the absorption bands at ~ 660 and 669 cm^{-1} to a specific vibrational mode of the *non-planar* (Np) and *planar* (P) cation conformers respectively. The intensities for these bands drastically change upon the occurrence of the observed phase transitions suggesting a competition between the two cation conformers as a function of temperature. To quantify the relative variation of the concentration of these two cation conformers, an analysis similar to those one previously carried out for the TFSI anion was performed for the bands due to cation conformers. The energy difference between the *planar* (P) and *non-planar* (Np) rotamers is obtained in the temperature range between 270 and 317 K (Fig. 7b). In this case r is the ratio between the intensities derived from the Lorentzian functions centered at ~ 660 and 669 cm^{-1} :

$$r = \frac{[C_P]}{[C_{\text{Np}}]} = \frac{I_{\text{Planar}}}{I_{\text{Non-Planar}}} = \frac{I_{669}}{I_{660}}. \quad (4)$$

The plot of the $\ln(r)$ vs. $1/T$ for all the spectra measured in the liquid phase on cooling and subsequently heating EDMIM-TFSI is reported in Fig. 7b. The slope of the linear regression provides a positive value of the enthalpy, equal to $5.98 \pm 0.31 \text{ kJ}\cdot\text{mol}^{-1}$, which is slightly larger than the calculated DFT energy difference. This result shows that the conformational distribution of the EDMIM cation is shifted on cooling toward the increase of

the lowest energy Np rotamer, while a drastically decrease of the P conformer concentration occurs in the sample. The analysis carried out is in accordance to what observed in the experimental spectra measured in the solid phase, where it can be noted that the increase in the intensity of the band at 660 cm^{-1} and the simultaneous reduction of the band at 669 cm^{-1} still exist even below the crystallization temperature showing a strong predominance of the *non-planar* conformer. Furthermore, in Fig. 7b for comparison are displayed the points of the $\ln(r)$ versus $1/T$ for the spectra measured on heating the sample at 304 and 324 K. These points, within the error, are consistent with the linear regression curve of the data measured on cooling the EDMIM-TFSI, suggesting that the conformational transition is a reversible process and consequently implies that both Np and P cation configurations are retained in the liquid phase. The redistribution of cation conformers is due to a change of the ethyl group, which can rotate along the C–N bond in order to obtain the stable configuration Np as consequence of temperature induced phase transition of EDMIM-TFSI sample. Modification of the local conformational structure originated by the rotation of the alkyl group induced by variation of thermodynamics variables such as temperature and pressure were observed in other imidazolium based ionic liquids [13–15, 46, 47]. Umebayashi et al. [35] were able to discriminate, with the support of the quantum chemical calculations, the *planar* and *non-planar* conformers of 1-ethyl-3-methylimidazolium and different anion such as BF_4^- , PF_6^- , CF_3SO_3^- and TFSI^- by considering characteristics bands in the range $200\text{--}500\text{ cm}^{-1}$ of the Raman spectrum. They found that the torsion energy difference calculated between the two cation isomers agree with the observed enthalpy energy of the conformational change, ΔH , showing in the liquid phase that the *non-planar* geometry is slightly favored in energy over the *planar* one and observing that conformational equilibrium is hardly influenced from the anionic environment. Lassègues et al. [42] analyzing Raman spectra of the 1-ethyl-3-methylimidazolium-TFSI showed that fast cooling quenches a metastable glassy phase composed of *planar* cation conformer, whereas slow cooling leads to a solid state composed of *non-planar* geometry, suggesting that 1-ethyl-3-methylimidazolium conformational state in the liquid phase is not strongly influenced by a bulky anion. Nevertheless, significant dependence of the conformational isomerism of 1-*n*-butyl-3-methylimidazolium cation from the halide anion were observed, reporting that the *gauche* conformer is stabilized by a stronger electrostatic field formed by smaller anions surrounding the cation. On the basis of our results, the conformational stability of the EDMIM-TFSI is strictly related to temperature effect involving CNCC dihedral angle changes of the ethyl group. At low temperatures, the flexibility of the alkyl side chain in the EDMIM cation promotes the formation of *non-planar* geometry, which along with the *trans* rotamer of TFSI anion lead to stabilize this ionic liquid in the solid phase.

5 Conclusions

In the present work we showed that alkyl chain length strongly affects the thermal properties and the structural organization of the imidazolium based-ionic liquids. We observed that the long aliphatic side chains lead HMIM-TFSI to form a glassy state at low temperatures, while, subsequently, on heating, a cold crystallizations process occurs and only the *cis* rotamer is retained. Conversely, shorter alkyl chain does not affect the phase transition for EDMIM-TFSI and the *trans* conformer results more stable in the solid phase. These results agree with our previous investigations performed for ammonium and pyrrolidinium cations with variable alkyl side chain length sharing the TFSI anion, therefore confirming

that the concentration of different conformer for this anion is strictly related to the length of the alkyl chain of the cation. Furthermore, the addition of a short polar chain on imidazolium cation drastically affect the ionic liquids thermal behavior, as shown by the analysis carried out on HOEMIM-TFSI, where no crystallization occurs, neither on cooling nor in heating, and both *cis* and *trans* conformers are present over the whole temperature range. Finally, our study reveals conformational changes of the EDMIM cation by means of the alkyl chain rotation occurring at the liquid–solid temperature phase transition. In particular, the markers of the occurrence of the lowest energy conformers were observed in the measured spectra. In accordance with DFT calculations the analysis of temperature dependence of these bands indicates that *non-planar* conformer is more stable than the *planar* one, and that both configurations are present in equilibrium in the liquid state, whereas in the solid phase the *non-planar* conformer is favored.

Supplementary Information The online version contains supplementary material available at <https://doi.org/10.1007/s10953-021-01079-2>.

Acknowledgements We wish to thank P. Roy and J.-B. Brubach for assistance at the AILES beamline of Synchrotron Soleil during beamtime #20170928 and #20190321. The beamtimes have received funding from the European Union's Horizon 2020 Research and Innovation programme under Grant Agreement No 730872 (CALIPSOplus).

References

1. Plechkova, N.V., Seddon, K.R.: Applications of ionic liquids in the chemical industry. *Chem. Soc. Rev.* **37**, 123–150 (2008)
2. Welton, T.: Ionic liquid in catalysis. *Coord. Chem. Rev.* **248**, 2459–2477 (2004)
3. Armand, M., Endres, F., MacFarlane, D.R., Ohno, H., Scrosati, B.: Ionic-liquid materials for the electrochemical challenges of the future. *Nat. Mater.* **8**, 621–629 (2009)
4. Chiappe, C., Pieraccini, D.: Ionic liquids: solvent properties and organic reactivity. *J. Phys. Org. Chem.* **18**, 275–295 (2005)
5. Navarra, M.A.: Ionic liquids as safe electrolyte components for Li-metal and Li-ion batteries. *Mater. Res. Soc. Bull.* **38**, 548–553 (2013)
6. Martinelli, A., Marechal, M., Östlund, Å., Cambedouzou, J.: Insights into the interplay between molecular structure and diffusional motion in 1-alkyl-3-methylimidazolium ionic liquids: a combined PFG NMR and X-ray scattering study. *Phys. Chem. Chem. Phys.* **15**, 5510–5517 (2013)
7. Russina, O., Triolo, A., Gontrani, L., Caminiti, R., Xiao, D., Hines Jr, G.L., Bartsch, R.A., Quitevis, E.L., Plechkova, N.V., Seddon, K.R.: Morphology and intermolecular dynamics of 1-alkyl-3-methylimidazolium bis{(trifluoromethane)sulfonyl}amide ionic liquids: structural and dynamic evidence of nanoscale segregation. *J. Phys. Condens. Matter* **21**, 424121–424129 (2009)
8. Triolo, A., Russina, O., Bleif, H.J., Di Cola, E.: Nanoscale segregation in room temperature ionic liquids. *J. Phys. Chem. B.* **111**, 4641–4644 (2007)
9. Navarra, M.A., Fujimura, K., Sgambetterra, M., Tsurumaki, A., Panero, S., Nakamura, N., Ohno, H., Scrosati, B.: New ether-functionalized morpholinium- and piperidinium-based ionic liquids as electrolyte components in lithium and lithium-ion batteries. *ChemSusChem* **10**, 2496–2504 (2017)
10. Zhou, Z.B., Matsumoto, H., Tatsumi, K.: Cyclic quaternary ammonium ionic liquids with perfluoroalkyltrifluoroborates: synthesis, characterization, and properties. *Chemistry*. **12**, 2196–2212 (2006)
11. Henderson, W.A., Young, V.G., Jr., Fox, D.M., De Long, H.C., Trulove, P.C.: Alkyl vs. alkoxy chains on ionic liquid cations. *Chem. Commun.* **35**, 3708–3710 (2006)
12. Li, H., Wang, Z., Chen, L., Wu, J., Huang, H., Yang, K., Wang, Y., Su, L., Yang, G.: Kinetic effect on pressure-induced phase transitions of room temperature ionic liquid, 1-ethyl-3-methylimidazolium trifluoromethanesulfonate. *J. Phys. Chem. B.* **119**, 14245–14251 (2015)
13. Yoshimura, Y., Takekiyo, T., Abe, H., Hamaya, N.: High-pressure phase behavior of the room temperature ionic liquid 1-ethyl-3-methylimidazolium nitrate. *J. Mol. Liq.* **206**, 89–94 (2015)

14. Chen, F., You, T., Yuan, Y., Pei, C., Ren, X., Huang, Y., Yu, Z., Li, X., Haiyan, Z., Pan, Y., Yang, K., Wang, L.: Pressure-induced structural transitions of a room temperature ionic liquid—1-ethyl-3-methylimidazolium chloride. *J. Chem. Phys.* **146**, 094502–094501 (2017)
15. Takekiyo, T., Imai, Y., Hatano, N., Abe, H., Yoshimura, Y.: Conformational preferences of two imidazolium-based ionic liquids at high pressures. *Chem. Phys. Lett.* **511**, 241–246 (2011)
16. Vitucci, F.M., Trequattrini, F., Palumbo, O., Brubach, J.-B., Roy, P., Paolone, A.: Infrared spectra of bis(trifluoromethanesulfonyl)imide based ionic liquids: experiments and ab-initio simulations. *Vib. Spectrosc.* **74**, 81–87 (2014)
17. Vitucci, F.M., Trequattrini, F., Palumbo, O., Brubach, J.-B., Roy, P., Navarra, M.A., Panero, S., Paolone, A.: Stabilization of different conformers of bis(trifluoromethanesulfonyl)imide anion in ammonium-based ionic liquids at low temperatures. *J. Phys. Chem. A* **118**, 8758–8764 (2014)
18. Palumbo, O., Trequattrini, F., Vitucci, F.M., Navarra, M.A., Panero, S., Paolone, A.: An Infrared spectroscopy study of the conformational evolution of the bis(trifluoromethanesulfonyl)imide ion in the liquid and in the glass state. *Adv. Condens. Matter Phys.* **2015**, 176067-1-176067-11 (2015)
19. Vitucci, F.M., Palumbo, O., Trequattrini, F., Brubach, J.-B., Roy, P., Meschini, I., Croce, F., Paolone, A.: Interaction of 1-butyl-1-methylpyrrolidinium bis(trifluoromethanesulfonyl)imide with an electrospun PVDF membrane: temperature dependence of the concentration of the anion conformers. *J. Chem. Phys.* **143**, 094707–094701 (2015)
20. Capitani, F., Gatto, S., Postorino, P., Palumbo, O., Trequattrini, F., Deutsch, O.M., Brubach, J.-B., Roy, P., Paolone, A.: The complex dance of the two conformers of bis(trifluoromethanesulfonyl)imide as a function of pressure and temperature. *J. Phys. Chem. B* **120**, 1312–1318 (2016)
21. Capitani, F., Trequattrini, F., Palumbo, O., Paolone, A., Postorino, P.: Phase transitions of PYR14-TFSI as a function of pressure and temperature: the competition between smaller volume and lower energy conformer. *J. Phys. Chem. B* **120**, 2921–2928 (2016)
22. Palumbo, O., Trequattrini, F., Appetecchi, G.B., Paolone, A.: Influence of alkyl chain length on microscopic configurations of the anion in the crystalline phases of PYR1A-TFSI. *J. Phys. Chem. C* **121**, 11129–11135 (2017)
23. Tsurumaki, A., Trequattrini, F., Palumbo, O., Panero, S., Paolone, A., Navarra, M.A.: The effect of ether-functionalisation in ionic liquids analysed by DFT calculation, infrared spectra, and Kamlet–Taft parameters. *Phys. Chem. Chem. Phys.* **20**, 7989–7997 (2018)
24. Palumbo, O., Trequattrini, F., Navarra, M.A., Brubach, J.-B., Roy, P., Paolone, A.: Tailoring the physical properties of the mixtures of ionic liquids: a microscopic point of view. *Phys. Chem. Chem. Phys.* **19**, 8322–8329 (2017)
25. Herstedt, M., Smirnov, M., Johansson, P., Chami, M., Grondin, J., Servant, L., Lassègues, J.C.: Spectroscopic characterization of the conformational states of the bis(trifluoromethanesulfonyl)imide anion (TFSI⁻). *J. Raman Spectrosc.* **36**, 762–770 (2005)
26. Martinelli, A., Matic, A., Johansson, P., Jacobsson, P., Borjesson, L., Fernicola, A., Panero, S., Scroscati, B., Ohno, H.: Conformational evolution of TFSI⁻ in protic and aprotic ionic liquids. *J. Raman Spectrosc.* **42**, 522–528 (2011)
27. Triolo, A., Russina, O., Fazio, B., Appetecchi, G.B., Carewska, M., Passerini, S.: Nanoscale organization in piperidinium-based room temperature ionic liquids. *J. Chem. Phys.* **130**, 164521–164526 (2009)
28. Zheng, W., Mohammed, A., Hines, L.G., Jr., Xiao, D., Martinez, O.J., Bartsch, R.A., Simon, S.L., Russina, O., Triolo, A., Quitevis, E.L.: Effect of cation symmetry on the morphology and physico-chemical properties of imidazolium ionic liquids. *J. Phys. Chem. B* **115**, 6572–6584 (2011)
29. Roy, P., GuidiCestelli, M., Nucara, A., Marcouille, O., Calvani, P., Giura, P., Paolone, A., Mathis, Y.-L., Gerschel, A.: Spectral distribution of infrared synchrotron radiation by an insertion device and its edges: a comparison between experimental and simulated spectra. *Phys. Rev. Lett.* **84**, 483–486 (2000)
30. Roy, P., Brubach, J.-B., Calvani, P., De Marzi, G., Filabozzi, A., Gerschel, A., Giura, P., Lupi, S., Marcouille, O., Mermet, A., Nucara, A., Orphal, J., Paolone, A., Vervloet, M.: Infrared synchrotron radiation: from the production to the spectroscopic and microscopic applications. *Nucl. Instrum. Methods Phys. Res., Sect. A* **467–468**, 426–436 (2001)
31. Shao, Y., Molnar, L.F., Jung, Y., Kussmann, J., Ochsenfeld, C., Brown, S.T., Gilbert, A.T., Slipchenko, L.V., Levchenko, S.V., O'Neill, D.P., DiStasio, R.A. Jr., Lochan, R.C., Wang, T., Beran, G.J., Besley, N.A., Herbert, J.M., Lin, C.Y., Van Voorhis, T., Chien, S.H., Sodt, A., Steele, R.P., Rassolov, V.A., Maslen, P.E., Korambath, P.P., Adamson, R.D., Austin, B., Baker, J., Byrd, E.F., Dachsel, H., Doerkson, R.J., Dreuw, A., Dunietz, B.D., Dutoi, A.D., Furlani, T.R., Gwaltney, S.R., Heyden, A., Hirata, S., Hsu, C.P., Kedziora, G., Khalliulin, R.Z., Klunzinger, P., Lee, A.M., Lee, M.S., Liang, W., Lotan, I., Nair, N., Peters, B., Proynov, E.I., Pieniazek, P.A., Rhee, Y.M., Ritchie, J., Rosta, E., Sherrill, C.D.,

- Simmonett, A.C., Subotnik, J.E., Woodcock, I.I.I., Zhang, H.L., Bell, W., Chakraborty, A.T., Chipman, A.K., Keil, D.M., Warshel, F.J., Hehre, A., Schaefer, W.J., Kong, I.I.I., H.F., Krylov, J., Gill, A.I., P. M., Head-Gordon, M.: Advances in methods and algorithms in a modern quantum chemistry program package. *Phys. Chem. Chem. Phys.* **8**, 3172–3191 (2006)
32. Hehre, W.J.: *A Guide to Molecular Mechanics and Quantum Chemical Calculations*. Wavefunction, Inc., Irvine (2003)
33. Umabayashi, Y., Mitsugi, T., Fukuda, S., Fujimori, T., Fujii, K., Kanzaki, R., Takeuchi, M., Ishiguro, S.: Lithium ion solvation in room-temperature ionic liquids involving bis(trifluoromethanesulfonyl) imide anion studied by Raman spectroscopy and DFT calculations. *J. Phys. Chem. B.* **111**, 13028–13032 (2007)
34. Fujii, K., Fujimori, T., Takamuku, T., Kanzaki, R., Umabayashi, Y., Ishiguro, S.: Conformational equilibrium of bis(trifluoromethanesulfonyl) imide anion of a room-temperature ionic liquid: raman spectroscopic study and DFT calculations. *J. Phys. Chem. B.* **110**, 8179–8183 (2006)
35. Umabayashi, Y., Fujimori, T., Sukizaki, T., Asada, M., Fujii, K., Kanzaki, R., Ishiguro, S.-I.: Evidence of conformational equilibrium of 1-ethyl-3-methylimidazolium in its ionic liquid salts: Raman spectroscopic study and quantum chemical calculations. *J. Phys. Chem. A* **109**, 8976–8982 (2005)
36. Blokhin, A.V., Paulechka, Y.U., Kabo., G.J.: Thermodynamic properties of [C6mim][NTf2] in the condensed state. *J. Chem. Eng. Data* **51**, 1377–1388 (2006)
37. Shimizu, Y., Ohte, Y., Yamamura, Y., Saito, K., Atake, T.: Low-temperature heat capacity of room-temperature ionic liquid, 1-hexyl-3-methylimidazolium bis(trifluoromethylsulfonyl)imide. *J. Phys. Chem. B.* **110**, 13970–13975 (2006)
38. Vitucci, F.M., Manzo, D., Navarra, M.A., Palumbo, O., Trequattrini, F., Panero, S., Bruni, P., Croce, F., Paolone, A.: Low temperature phase transitions of 1-butyl-1-methylpyrrolidinium bis(trifluoromethanesulfonyl)imide swelling a PVdF electrospun membrane. *J. Phys. Chem. C* **118**, 5749–5755 (2014)
39. Maria Moschovi, A., Dracopoulos, V.: Structure of protic (HCnImNTf2, n = 0–12) and aprotic (C1Cn-ImNTf2, n = 1–12) imidazolium ionic liquids: a vibrational spectroscopic study. *J. Mol. Liq.* **210**, 189–199 (2015)
40. Holbrey, J.D., Reichert, W.M., Rogers, R.D.: Crystal structures of imidazolium bis(trifluoromethanesulfonyl)imide “ionic liquid” salts: the first organic salt with a cis-TFSI anion conformation. *Dalton Trans.* **15**, 2267–2271 (2004)
41. Choudhury, A.R., Winterton, N., Steiner, A., Cooper, A.L., Johnson, K.A.: In situ crystallization of ionic liquids with melting point below – 25 °C. *CrystEngComm.* **8**, 742–745 (2006)
42. Lassègues, J.C., Grondin, J., Holomb, R., Johansson, P.: Raman and ab initio study of the conformational isomerism in the 1-ethyl-3-methylimidazolium bis(trifluoromethanesulfonyl)imide ionic liquid. *J. Raman Spectrosc.* **38**, 551–558 (2007)
43. Zhang, S., Qi, X., Ma, X., Lu, L., Zhang, Q., Deng, Y.: Investigation of cation–anion interaction in 1-(2-hydroxyethyl)-3-methylimidazolium-based ion pairs by density functional theory calculations and experiments. *J. Phys. Org. Chem.* **25**, 248–257 (2012)
44. Zhang, S., Qi, X., Ma, X., Lu, L., Deng, Y.: Hydroxyl ionic liquids: the differentiating effect of hydroxyl on polarity due to ionic hydrogen bonds between hydroxyl and anions. *J. Phys. Chem. B.* **114**, 3912–3920 (2010)
45. Fakhraee, M., Zandkarimi, B., Salari, H., Gholami, M.R.: Hydroxyl-Functionalized 1-(2-hydroxyethyl)-3-methylimidazolium ionic liquids: thermodynamic and structural properties using molecular dynamics simulations and ab initio calculations. *J. Phys. Chem. B.* **118**, 14410–14428 (2014)
46. Ozawa, R., Hayashi, S., Saha, S., Kobayashi, A., Hamaguchi, H.: Rotational isomerism and structure of the 1-butyl-3-methylimidazolium cation in the ionic liquid state. *Chem. Lett.* **32**, 948–949 (2003)
47. Chang, H.-C., Jiang, J.-C., Su, J.-C., Chang, C.-Y., Lin, S.H.: Evidence of rotational isomerism in 1-butyl-3-methylimidazolium halides: a combined high-pressure infrared and Raman spectroscopic study. *J. Phys. Chem. A* **111**, 9201–9206 (2007)